11th World Congress on Computational Mechanics (WCCM XI)
5th European Conference on Computational Mechanics (ECCM V)
6th European Conference on Computational Fluid Dynamics (ECFD VI)
E. Oñate, J. Oliver and A. Huerta (Eds)

A ROBUST TIME INTEGRATION FOR DYNAMIC INTERACTION OF HIGH-SPEED TRAIN AND RAILWAY STRUCTURE INCLUDING DERAILMENT DURING AN EARTHQUAKE

M. TANABE[*], M. SOGABE[†], H. WAKUI[†], N. MATSUMOTO[†] AND Y. TANABE[+]

[*] Kanagawa Institute of Technology
Atsugi, Kanagawa, 243-0292, Japan
e-mail: tanabe@sd.kanagawa-it.ac.jp

[†] Railway Technical Research Institute
Kokubunji, Tokyo, 185-8540, Japan
e-mail: sogabe@rtri.or.jp, wakui@rtri.or.jp, nobel@rtri.or.jp

[+] Laboratory for Computational Mechanics Inc.
3-14-18 Kurihara Chuo, Zama, 252-0014, Japan

Key Words: *Exact time integration, Dynamic interaction, Train, derailment, Earthquake*

Abstract. In this paper a robust and efficient computational method to solve for the dynamic interaction of a high-speed train and railway structure including derailment during an earthquake is given. The motion of the train is modeled in multibody dynamics. Mechanical models to express contact-impact behaviors between wheel and rail before derailment and between wheel and the track structure after derailment are described to solve the interaction during an earthquake. The motion of railway structure is modeled with various finite elements. Modal reduction has been developed to solve nonlinear equations of the combined motion of the train and railway structure effectively. A robust time integration using an exact time integration in the modal coordinate has been developed to avoid a round-off error appeared in the numerical time integration for a very small time increment to solve the interaction including derailment during an earthquake. Some examples are demonstrated.

1 INTRODUCTION

When a high-speed train runs on the railway structure during an earthquake, there is a radical dynamic interaction between the train and railway structure. The huge impact force between wheel and rail creates lifting of wheel, derailment and post-derailment behavior during a strong earthquake. What is difficult of the phenomenon to solve is that it shows a high-frequency response higher than several hundred Hz due to the impact between the train and railway structure during an earthquake that is mixed with a low-frequency fundamental response less than about 20 Hz depending on the railway structure. This is the so-called multiscale phenomenon of frequency in the interaction of the train and railway sturucture

during an earthquake. The time increment Δt to solve for the interaction including derailment becomes very small for the convergency in the nonlinear iterations during each time increment that may cause a round-off error in the numrical time integration since the lower natural frequency of the railway structure with the large mass of the base ground from which an earthquake wave enters attached to it and huge terms in the order of $1/\Delta t^2$ are included in the dynamic stiffness in the numerical time integration. To avoid the round-off error for the very small time increment in the numerical integration in the dynamic problem, the scaling techniquie has been developed [1] .

Computational methods to solve for the dynamic interaction of a high-speed train and railway structure have been developed by using mutibody dynamics together with finite element method, and various mechanical models for the car, the railway structure and the interaction models between wheel and rail have been developed based on the purposes and applications to design railways [2-5]. However, very little work related to derailment and post-dearilment behaviors of the train on the railway structure during an earthquake has been reported so far [6-7].

In this paper a robust and efficient computational method to solve for the dynamic interaction of a high-speed train and railway structure including derailment and post-derailment behaviors during an earthquake is given. The motion of the train is modeled in multibody dynamics where nonlinear springs and dampers are used to connect all components [7]. Mechanical models to express contact-impact behaviors between wheel and rail before derailment and between wheel and the track structure after derailment are given to solve the interaction during an earthquake effectively.

The motion of railway structure is modeled with various finite elements. Modal reduction has been developed to solve nonlinear equations of the combined motion of the train and railway structure during an earthquake effectively. A robust time integration using an exact time integration in the modal coordinate has been developed to solve the radical dynamic interaction to avoid the round-off error which appears in the numerical time integration such as the Newmark method for a very small time increment needed.

Based on the present method a computer program, DIASTARS, has been developed to solve the dynamic interaction of a Shinkansen train (high-speed train in Japan) and railway structure including derailment during an earthquake. Numerical examples are demonstrated.

2 INTERACTION BETWEEN WHEEL AND TRACK STRUCTURE

2.1 Contact between wheel and rail before derailment

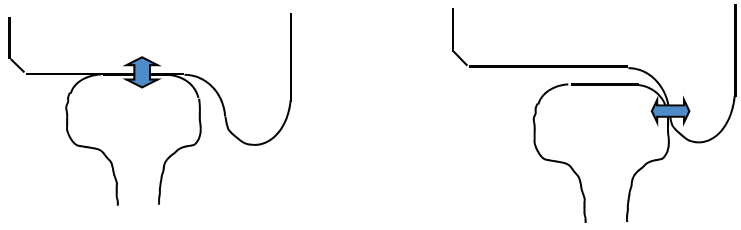

(a) Vertical direction (b) Transverse direction

Fig. 1 Contact modes between wheel and rail

Assuming that the yawing and rolling of wheel-set are relatively small for the contact behavior between wheel and rail considered here, two dimensional geometries of the cross sections of wheel and rail are considered, and the contact-impact behavior in the normal direction on the contact surface between wheel and rail is modeled simply in two modes of the contact in the vertical and transverse directions as shown in Fig. 1.

Assuming that wheel and rail are stiff enough, regarding the vertical mode of the contact the contact displacement between wheel and rail in the vertical direction, δ_Z, is expressed as a function of displacements of the rail z_R and the wheel z_w in the vertical direction and also the relative displacement on the contact surface between wheel and rail in the transverse direction d_y depending on the geometry of the rail and wheel as follows

$$\delta_Z = \delta_Z(z_R, z_W, d_y) . \tag{1}$$

The contact displacement δ in the normal direction on the contact surface between wheel and rail is obtained from the contact angle at the contact position. When wheel contacts on rail, there is a contact force created on the contact surface. The contact force on the contact surface between wheel and rail in the normal direction, H, is expressed as a function of δ and d_y as

$$H = H(\delta, d_y) . \tag{2}$$

Regarding the transverse mode of the contact between wheel and rail, the contact displacement in the transverse direction δ_y is also expressed as a function of d_y and δ_Z depending on the geometry of the cross sections of wheel and rail as

$$\delta_y = \delta_y(d_y, \delta_Z) . \tag{3}$$

When a wheel contacts on the rail in the transverse direction, the contact force is obtained in the same manner as the contact mode in the vertical direction described above.

Regarding the tangential and longitudinal directions on the contact surface between wheel and rail, constitutive equations to describe the relationship between creep forces and slipping rates of wheel are given [9]. The creep force in the tangential direction Q_c on the contact surface between wheel and rail are described mathematically here as functions of slipping rates of wheel in the longitudinal and tangential directions, S_x and S_t, and also of the spin rate around the normal vector on the contact surface, S_n, as [10]

$$Q_c = Q_c(S_x, S_t, S_n) \tag{4}$$

2.2 Derailment Criterion

When the relative displacement between wheel and rail in the transverse direction, d_y, exceeds derailment criterions u_{d1} or u_{d2}, it is detected that the derailment in the field side or gauge side is initiated, respectively as shown in Fig. 2 that leads to the post-derailment behavior of the wheel on the track structure. After derailment of wheel from rail during an earthquake the wheel touches down on the track structure .

(a) Field-side derailment (b) Gauge-side derailment

Fig. 2 Derailment criterion of left wheel

2.3 Contact-impact behavior between wheel and track structure after derailment

1) Contact-impact behavior in the vertical direction after derailment

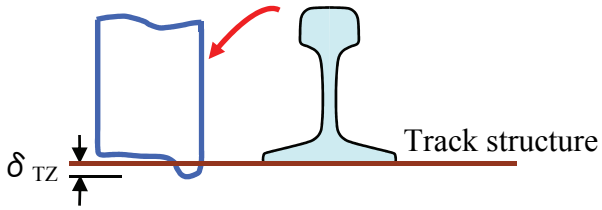

Fig. 3 Vertical relative displacement between wheel and track structure δ_{TZ}

When a wheel touches down on the track surface after derailment as shown in Fig.3, the impact force of the wheel on the track structure on the contact surface, Q_{TZ}, is given here as a function of the relative displacement between wheel and the track structure in the vertical direction, δ_{TZ} depending on material properties of the contact between wheel and the track structure as

$$Q_{TZ} = Q_{TZ}(\delta_{TZ}) \tag{5}$$

2) Contact-impact behavior in the lateral direction after derailment

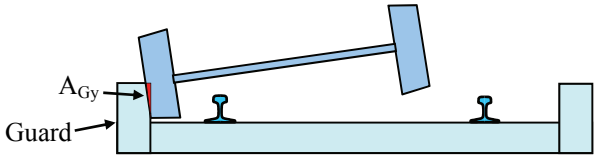

Fig. 4 Contact between wheel and guard on the track structure in the transverse direction

Guards are attached on the track structure to prevent wheel deviating from the track after derailment during an earthquake to build an earthquake-safe railway system as shown in Fig. 4. After the derailment of a wheel, it contacts on the guard of the track structure in the transverse direction. The contact force Q_{Gy} is expressed here as a function of the embedded area A_{Gy} between the wheel and the guard as

$$Q_{Gy} = Q_{Gy}(A_{Gy}). \tag{6}$$

If the guard has an enough height and strength for the impact force between wheel and guard, the wheel is guided well between left and right guards in the rail direction after the derailment preventing wheel deviating from the track during an earthquake.

3 EQUATION OF MOTION OF THE TRAIN AND RAILWAY STRUCTURE

3.1 Equation of motion of the train

The motion of the train is modeled in multibody dynamics with nonlinear springs and dampers used to connect all components [8]. Assuming that the train runs at a constant speed, the equation of 3D motion of the train is derived and written in a familiar matrix form as

$$M^v \ddot{X}^v + D^v(\dot{X}^v) + K_0^v X^v + K_N^v(X^v) = F^v \tag{7}$$

where X^v and F^v are displacement and load vectors of the train, M^v is the mass matrix, $D^v(\dot{X}^v)$ is the damping force vector, and K_0^v is the linear stiffness matrix and K_N^v is the nonlinear term in the internal force vector, respectively. Note that the damping force vector is nonlinear depending on the velocity vector, the nonlinear term in the stiffness matrix depends on the displacement vector of the train, and F^v is a nonlinear force vector due to the interaction between wheel and the track structure depending on displacement and velocity vectors of the train and railway structure.

3.2 Equation of motion of railway structure

A railway structure is modeled with various finite elements. Assembling all elements in the model, the equation of motion of a railway structure is obtained and written in a familiar matrix form as

$$M^b \ddot{X}^b + D^b(\dot{X}^b) + K_0^b X^b + K_N^b(X^b) = F^b \tag{8}$$

where X^b and F^b are the displacement and load vectors of the railway structure, and M^b is the mass matrix, $D^b(\dot{X}^b)$ is the damping force vector, and K_0^b is the linear stiffness matrix and K_N^b is nonlinear term in the internal force vector, respectively. Note that the nonlinear term in the stiffness matrix depends on the displacement vector of the railway structure, and F^b is a nonlinear force vector due to the interaction between wheel and the track structure depending on displacement and velocity vectors of the train and railway structure.

4 NUMERICAL METHOD

4.1 Modal reduction

A modal reduction is applied to displacement vectors of the train and the railway structure as

$$X^{v} = \Phi^{v} Z^{v} \tag{9}$$
$$X^{b} = \Phi^{b} Z^{b} \tag{10}$$

where Φ^{v} and Φ^{b} are rectangular matrices made of the mode vectors of the train and railway structure, and Z^{v} and Z^{b} are the modal coordinates, respectively. Moving the nonlinear terms in eqs. (7) and (8) to the right sides of equations, and operating the modal transformation by Φ^{v} and Φ^{b} respectively, equations of motions of the train and the railway structure are derived in the modal coordinates as

$$\ddot{Z}^{v} + [(\omega_i^{v})^2] Z^{v} = \widetilde{F}^{v} \tag{11}$$
$$\ddot{Z}^{b} + [(\omega_i^{b})^2] Z^{b} = \widetilde{F}^{b} \tag{12}$$

where ω_i^{v} and ω_i^{b} are angular frequencies of i-th mode in the train and railway structure, respectively, and $[(\omega_i^{v})^2]$ denotes a diagonal matrix with i-th diagonal element of $(\omega_i^{v})^2$ where

$$\widetilde{F}^{v} = (\Phi^{v})^{T} (F^{v} - D^{v}(\dot{X}^{v}) - K_N^{v}(X^{v})) \tag{13}$$
$$\widetilde{F}^{b} = (\Phi^{b})^{T} (F^{b} - D^{b}(\dot{X}^{b}) - K_N^{b}(X^{b})) \tag{14}$$

However, the superscript T denotes the transpose of the matrix. Note that all nonlinear terms for the train and railway structure are included in $\widetilde{F}^{v}$ in eq. (13) and $\widetilde{F}^{b}$ in eq.(14), respectively.

4.2 Exact time integration

Now assume that solutions of eqs. (11) and (12) were obtained at time t, then we have the following type of equation to be solved at time t+s for each mode as

$$\ddot{z}^{v}_{t+s} + \omega^2 z_{t+s} = f(s, z_{t+s}) \tag{15}$$

where s is the time increment from time t such that $0 \le s \le \Delta t$, $f(s, z_{t+s})$ is a nonlinear function depending on s and z. Approximating the right-hand side in eq.(15) with m-th degree of polynomial, we have the exact time integration to the equation at time t+Δt since the numerical time integration causes a round-off error for very small time increments needed to solve the radical dynamic interaction in the derailment during an earthquake. However, since the equations are strongly nonlinear, iterative calculations are needed during each time increment until the unbalanced force between the train and railway structure becomes small enough within a tolerance specified.

5 NUMERICAL EXAMPLES

5.1 One dimensional nonlinear dynamic problem

Fig. 5 shows a one dimensional nonlinear dynamic problem with the natural frequency of ω, damping constant of h and the gravity force of g due to the unit mass where a contact element with the gap G and the contact spring constant K is attached.

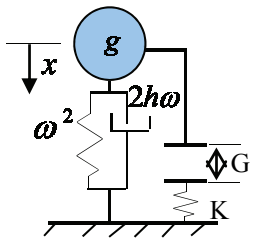

Fig. 5 One dimensional nonlinear dynamic problem

The exact time integration is applied to the problem with $\omega = 2\pi/10$ rad/sec, h=0.1, $K = 5\times10^3$ N/m, G=0.03m and g=9.8N where the linear approximation (m=1) to the right-hand side of the equation of motion is made. The displacement response by the exact time integration shows quite a good agreement with the closed form solution for very small time increments of both $\Delta t = 10^{-6}$ and 10^{-8}(sec.) . The numerical time integration by Newmark method failed due to the round-off error for very small time increments of both $\Delta t = 10^{-6}$ and 10^{-8}.

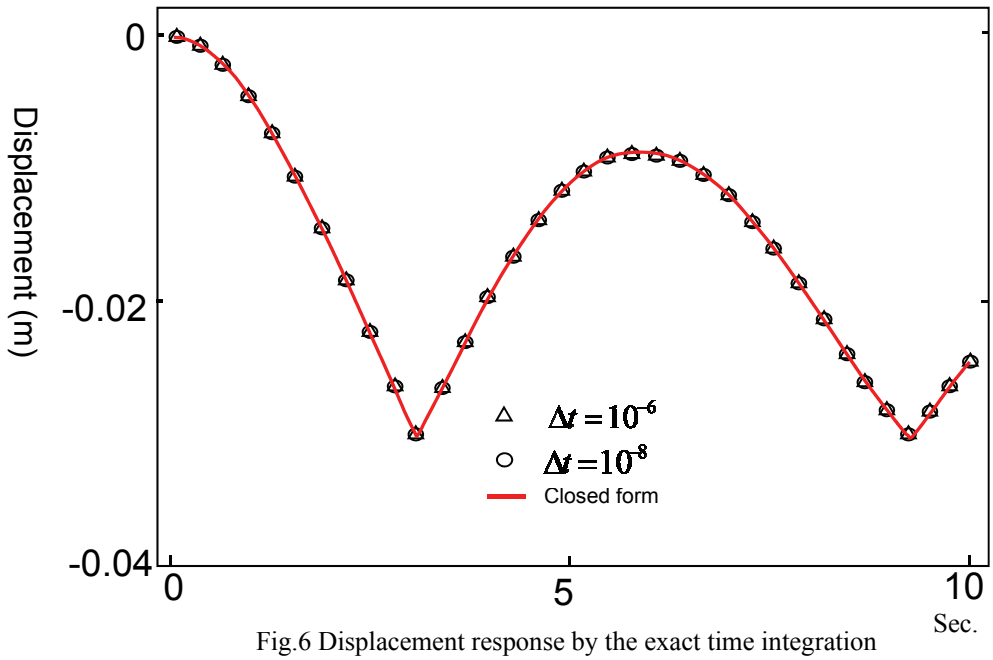

Fig.6 Displacement response by the exact time integration

5.2 Simulation of a Shinkansen car running on the viaduct with guards attached during an earthquake

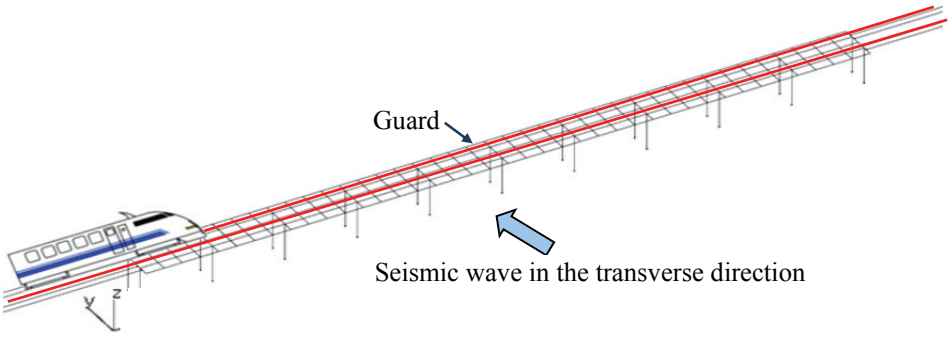

(a) Railway structure modeled with shell and beam elements

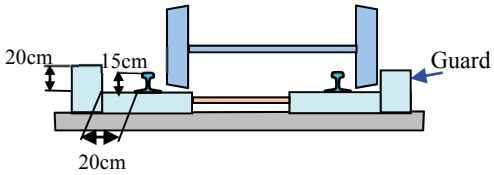

(b) Cross section of the ladder track with guards attached

Fig. 7 A Shinkansen car on the ladder track with guards attached on a 10 spanned viaduct during an earthquake

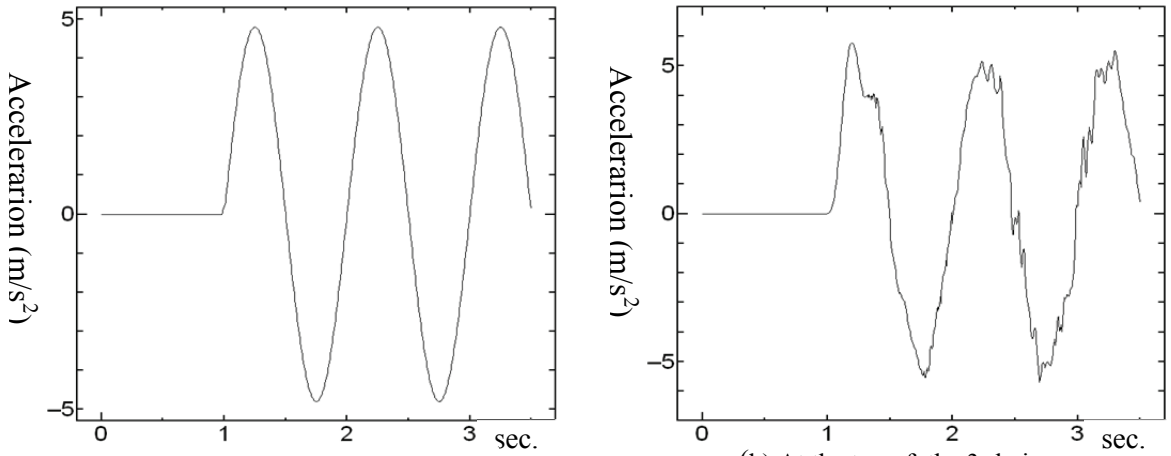

(a) At the base of the 3rd pier (b) At the top of the 3rd pier

Fig. 8 Transverse acceleration of the 3rd pier

Based on the present method, the simulation of a Shinkansen car running at a speed of 200km/h during an earthquake on the ladder track of 10 spanned viaduct with the height of 10m, the span-length of 8m and the width of 11.6 m as shown in Fig. 7 has been conducted. The ladder track is made of ladder-shaped composite concrete beams to support rails tied with steel pipes where guards are attached as shown in Fig.7b to prevent wheel deviating from the

track even after derailment during a strong earthquake [11-12]. A sinusoidal seismic wave with the maximum acceleration of 4.80 m/sec^2, the wave number of three, and the frequency of 1Hz was given from the basis of all piers in the transverse direction. The frequency of 1Hz is close to the resonance frequency of rolling motion of the car body, truck and wheel-set leading to derailment of wheel from the rail. The frame structure of the viaduct is modeled with beam elements and the concrete slab with shell elements.

Fig. 8 shows transverse acceleration at the base and top of the 3rd pier, respectively. The maximum acceleration at the top of the pier is amplified about 25% to the maximum acceleration of 4.8 m/s^2 given from the base. Fig. 9 shows the vertical displacement response of the right wheel at the 1st wheel-set. It is shown that the wheel runs onto the rail due to the impact between wheel and rail in the vertical direction, derails, touches down on the track,

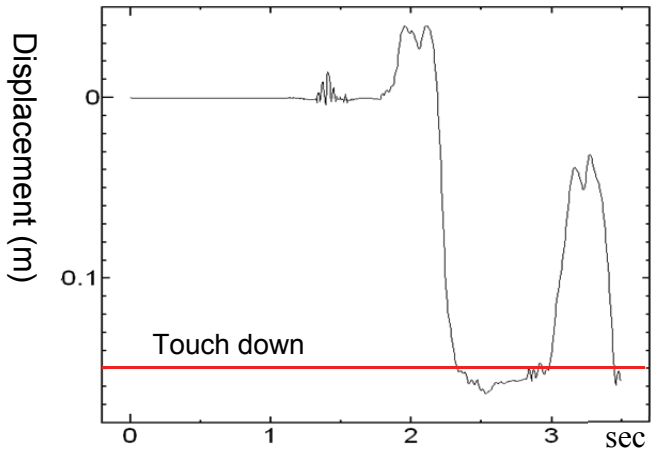

Fig. 9 Vertical displacement of the right wheel

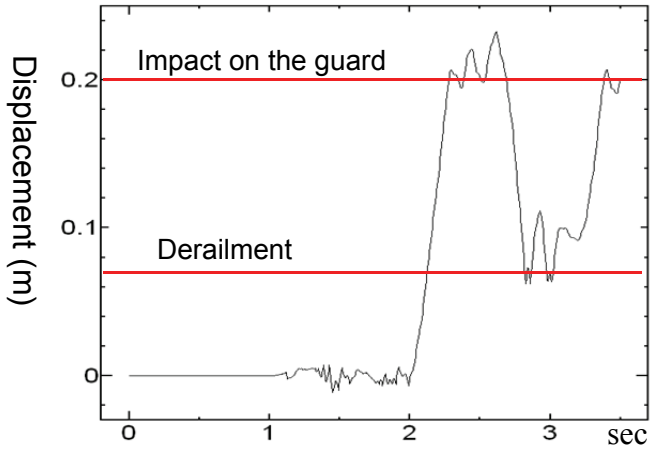

Fig. 10 Relative displacement between the right wheel and rail in the transverse direction

and lifts on the track surface during the earthquake. Fig. 10 shows the relative displacement response between the right wheel and rail in the transverse direction, δ_y, at the 1st wheel-set. When δ_y exceeds u_{d1} (7cm) shown in Fig.2, the derailment to the field side is initiated, the wheel touches down on the surface of the ladder track in the vertical direction, impacts on the guard of the track in the transverse direction, rebounds and gets back to the rail without deviating from the track. The track with the guards attached was shown to be effective to prevent the wheel deviating from the track even after derailment during the earthquake.

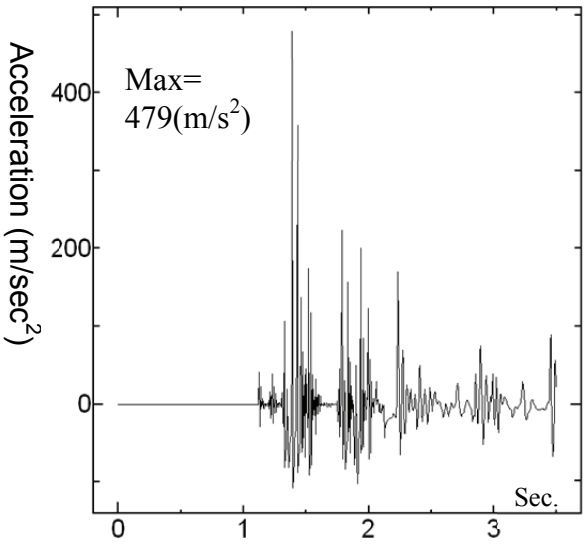

Fig. 11 Transverse acceleration of 1st wheelset

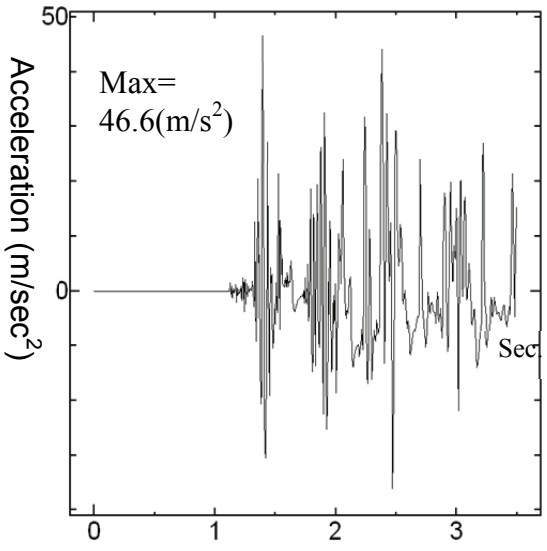

Fig. 12 Transverse acceleration of 1st truck

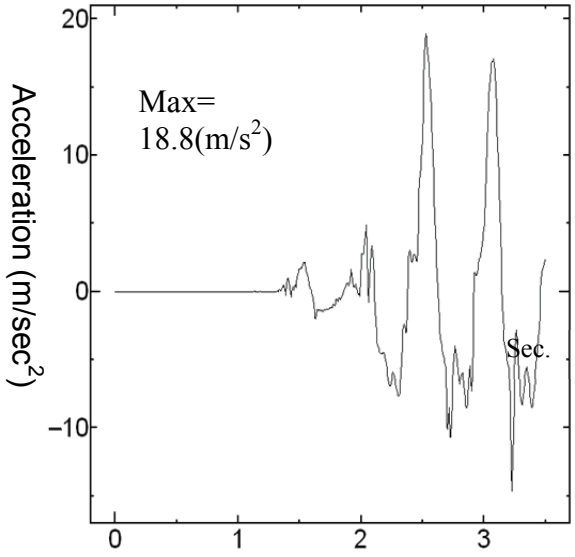

Fig. 13 Transverse acceleration of car body

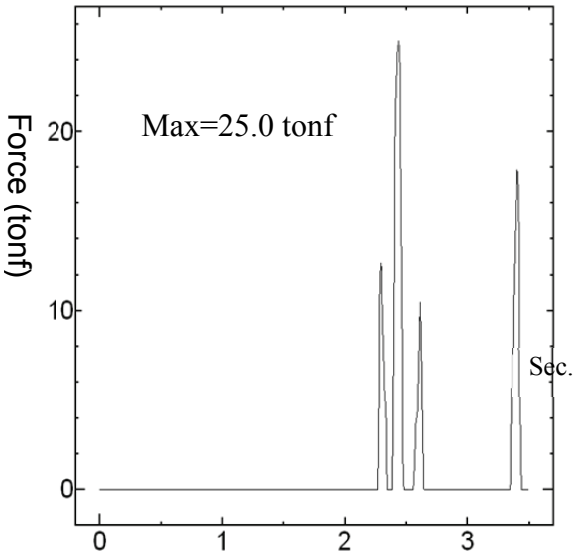

Fig. 14 Impact force of the right wheel on the guard in the transverse direction

Fig.11, 12 and 13 show the transverse acceleration of the 1st wheel-set, the 1st truck and the car body. The maximum acceleration of 479 m/s^2 at the wheelset is shown to be largely reduced to 46.6 m/s^2 at the truck and 18.8 m/s^2 at the car body.

Fig.14 shows the impact force of the right wheel on the guard. The maximum impact force of the wheel on the guard is shown to be about 25 tonf during the earthquake.

6 CONCLUSIONS

A robust and efficient computational method to solve for the dynamic interaction of a high-speed train and railway structure including derailment during an earthquake was given. Efficient mechanical models to solve contact-impact behaviors between wheel and the track structure including derailment were described. Modal reduction was applied to equations of motions of train and railway structures to solve for the interaction effectively. A robust time integration using the exact time integration has been developed to avoid the round-off error occurred in the numerical time integration for very small time increments needed to solve the radical dynamic interaction between wheel and track structure during an earthquake. Simulation of a Shinkansen car on the 10 spanned viaduct including derailment and post derailment behaviors during an earthquake was demonstrated. The computational method developed here would be effective to design an earthquake-safe railway system.

REFERENCES

[1] O. A. Bauchau, A. Epple and C. L. Bottasso, Who's afraid of high index DAES? Scaled and augmented Lagrangian formulations in multibody dynamics, *8th World Congress on Computational Mechanics*, Venice, Italy, 2008.

[2] M. Tanabe, H. Wakui and N. Matsumoto, The finite element analysis of dynamic interactions of high-speed Shinkansen, rail, and bridge, *Computers in Engineering,* Book No. G0813A, 17-22, ASME, 1993.

[3] A. Jaschinski, G. Schupp and H. Netter, Demonstration of simulation potentials in railway vehicle system dynamics through selected examples, *Proceedings of World Congress on Railway Research*, vol. D, 15-23, 1997.

[4] S. Bruni, A. Collina, R. Corradi and G. Diana, Numerical simulation of train-track-structure interaction for high speed railway systems, *Proceedings of Structures for High-Speed Railway Transportation*, *IABSE Symposium*, Antwerp, Belgium, 2003.

[5] R. Simoes, R. Calcada and R. Delgado, Track-bridge interaction in railway lines: Numerical modeling and application, *Track-Bridge Interaction on High-Speed Railways*, 205-216, FEUP Porto Portugal, 2007.

[6] M. Tanabe, N. Matsumoto, H. Wakui, M. Sogabe, H. Okuda and Y. Tanabe, A simple and efficient numerical method for dynamic interaction analysis of a high-speed train and railway structure during an earthquake, J. Computational and Nonlinear Dynamics, Vo.3/ 041002, ASME, 2008.

[7] M. Tanabe, N. Matsumoto, H. Wakui, M. Sogabe, Simulation of a Shinkansen train on the railway structure during an earthquake, *Japan J. Indust. Appl. Math.,* 28, 223-236, 2011.

[8] M. Tanabe, S. Komiya, H. Wakui, N. Matsumoto and M. Sogabe, Simulation and visualization of a high-speed Shinkansen train on the railway structure, *Japan J. Indust. Appl. Math.* vol.17, 309-320, 2000.
[9] J. J. Kalker, *Three-dimensional elastic bodies in rolling contact,* Kluwer, 1990.
[10] *Dynamics of railway vehicle,* JSME, 1994.
[11] H. Wakui, Technological innovation in railway structure system with ladder sleeper, *Concrete Journal,* Vol.36, No.5, 8-16, 1998.
[12] K. Asanuma, M. Sogabe, T. Watanabe, J. Okayama and H. Wakui, Development of a Ballasted ladder track equipped with a vehicle guide device, *RTRI Report* Vol.23, No.2, 27-32, 2009.